The Crystal structure of human GLRX5: iron sulphur cluster coordination, tetrameric assembly and monomer activity

Catrine Johansson, Annette K Roos, Sergio J Montano, Rajib Sengupta, Panagis Filippakopoulos, Kunde Guo, Frank von Delft, Arne Holmgren, Udo Oppermann, Kathryn L Kavanagh

Biochemical Journal Immediate Publication. Published on 29 Oct 2010 as manuscript BJ20101286

THE CRYSTAL STRUCTURE OF HUMAN GLRX5: IRON SULPHUR CLUSTER COORDINATION, TETRAMERIC ASSEMBLY AND MONOMER ACTIVITY

Catrine Johansson[*1], Annette K. Roos[*‡], Sergio J Montano[†], Rajib Sengupta[†], Panagis Filippakopoulos[*], Kunde Guo[*], Frank von Delft[*], Arne Holmgren[†], Udo Oppermann[*§], Kathryn L. Kavanagh[*]

[*] Structural Genomics Consortium, University of Oxford, Old Road Campus Research Building, Roosevelt Drive, Oxford, OX3 7DQ United Kingdom.
[†]Department of Medical Biochemistry and Biophysics, Karolinska Institute, SE 171 77 Stockholm, Sweden.
[‡]Current address: Dept. of Cell and Molecular Biology, Uppsala University, Biomedical Center, Box 596, SE-751 24 Uppsala, Sweden,
[§] Oxford Biomedical Research Unit, Botnar Research Center, Oxford, OX3 7LD, United Kingdom

Key words: glutaredoxin, iron-sulphur, glutathione, crystallisation, Ribonucleotide reductase, analytical ultracentrifugation

Abbreviations: GLRXs, glutaredoxins; FeS, iron-sulphur; GSH, glutathione; GSSG, glutathione disulfide; IRP1, iron-regulatory protein 1;ISA, iron-sulphur assembly; ISC, iron-sulphur cluster; IRE, iron response element; TXNRD, thioredoxin reductase; TXN, thioredoxin; GR, glutathione reductase; RNR, ribonucleotide reductase.

[1]To whom correspondance should be adressed: Catrine Johansson, Structural Genomics Consortium, Botnar Research Centre, University of Oxford, UK, Fax: +44 1865 737231, E-mail: catrine.johansson@sgc.ox.ac.uk

Running title: Crystal structure of human GLRX5

SYNOPSIS

Human glutaredoxin 5 (GLRX5) is an evolutionarily conserved thiol-disulfide oxidoreductase that has a direct role in the maintenance of normal cytosolic and mitochondrial iron homeostasis and its expression affects haem biosynthesis and erythropoiesis. We have crystallised the human GLRX5 bound to two [2Fe2S] clusters and four glutathione (GSH) molecules. The crystal structure revealed a tetrameric organisation with the [2Fe2S] clusters buried in the interior and shielded from the solvent by the conserved β1-α2 loop, Phe69 and the GSH molecules. Each [2Fe2S] cluster is ligated by the N-terminal active site cysteine (Cys67) thiols contributed by two protomers and two cysteine thiols from two GSH. The two subunits coordinating the cluster are in a more extended conformation compared to FeS-bound human GLRX2 and the intersubunit interactions are more extensive and involve conserved residues among monothiol GLRXs. Gelfiltration chromatography and analytical ultracentrifugation supported a tetrameric organisation of holo GLRX5 while the apo protein is monomeric. Mass spectrometry analyses revealed glutathionylation of the cysteines in the absence of the [2Fe2S] cluster, which would protect them from further oxidation and possibly facilitate cluster transfer/acceptance. Apo GLRX5 reduced glutathione mixed disulfides with a rate 100 times slower than GLRX2 and was active as a glutathione-dependent electron donor for mammalian ribonucleotide reductase.

INTRODUCTION

Glutaredoxins (GLRXs) are small evolutionarily conserved thiol-disulfide oxidoreductases that are involved in the maintenance of cellular redox homeostasis and in cellular redox signalling. Recently GLRXs have also been implicated in the maintenance of cytosolic and mitochondrial iron homeostasis and proteins from different organisms have been shown to coordinate [2Fe2S] clusters [1-6].

Structurally, GLRXs belong to the thioredoxin fold superfamily of proteins but are distinguished from the thioredoxins by their specificity for glutathione (GSH). Depending on the number of cysteine residues in the active site sequence they can be divided into monothiol (CGFS) and dithiol (CP/SYC) GLRXs. Dithiol GLRXs are efficient catalysts of protein disulfide reactions, especially in reduction of mixed disulfides with glutathione. They have been shown to protect cells from oxidative stress and apoptosis, to regulate transcription factors and have through these processes been implicated in several disease-related conditions [7]. Monothiol GLRXs show a higher degree of sequence identity compared to the dithiol GLRXs and can in eukaryotes be further categorized into single-domain and multi-domain proteins. Some monthiol GLRXs have a five amino acid insertion in the loop preceding the active site as well as a WP motif with unknown function. They contain several conserved amino acids known to be involved in GSH binding but have low or no measurable activity in assays using established model substrates for glutaredoxins [8-10]. Alternatively, monothiol GLRXs have been implicated in iron regulation [9, 11-14] and iron-sulphur cluster biogenesis[15]. Hence, monothiol GLRXs are structurally similar but biochemically different from dithiol GLRXs.
To date four GLRXs have been identified in the human genome: two dithiol GLRXs, GLRX1 and GLRX2, a multi-domain monothiol GLRX3 [16] and the mitochondrial single-domain monothiol GLRX5. In addition, there are two thioredoxin reductases (TXNRDs) with an N-terminal GLRX domain (TXNRD3 and TXNRD1 v_3)[17]. Human GLRX5 is well conserved among eukaryotes and initial studies in yeast revealed early an important role in mitochondrial FeS cluster biogenesis [11]. Phylogenetic profiling predicts that GLRX5 is part of the ISC iron-sulphur assembly machinery[18] and it is suggested to be required for transfer and insertion of clusters into acceptor proteins after the clusters have been assembled on the ISCU scaffold protein [19]. In addition, yeast two-hybrid experiments demonstrate that GLRX5 interacts with the ISA1 scaffold protein [18]. Recently, Wingert *et al*. showed that deficiency of the GLRX5 ortholog in zebrafish (known as Shiraz) affects haem biosynthesis through a cytosolic iron regulatory protein (IRP1)[15]. In humans, a silent mutation in the *glrx5* gene that results in decreased levels of GLRX5 protein, results in sideroblastic-like microcytic anemia characterised by mitochondrial iron overload and impaired haem synthesis [20].

Here we describe the crystal structure of the [2Fe2S]-bound human GLRX5 and present a biochemical characterisation of the protein. Our results reveal a tetrameric organisation with pronounced differences in the lability or accessibility of the [2Fe2S] cluster compared to human GLRX2 and show that the apo protein possesses low but significant GSH-disulfide oxidoreductase activity.

EXPERIMENTAL

Expression and purification of recombinant human GLRX2 and GLRX5

Recombinant human GLRX2 was expressed and purified as described previously [6]. A template plasmid encoding full length human GLRX5 was obtained from the Mammalian Gene Collection (cDNA clone IMAGE:6066312). A construct comprising residue 35-148, lacking the N-terminal mitochondrial signal, was cloned into pNIC28-Bsa4 (GenBank accession EF198106) with a

Tobacco Etch Virus (TEV) cleavable N-terminal His_6 tag. For expression of native GLRX5, the plasmid was transformed into a phage-resistant derivative of *Escherichia coli (E.coli)* strain BL21(DE3) carrying the pRARE2 plasmid for rare codon expression. The cells were grown at 37 °C in Terrific Broth supplemented with 50 µg/mL kanamycin and 34 µg/mL chloramphenicol, until the culture reached an OD_{600} of 1.5. The temperature was decreased to 18 °C and protein expression was induced with 0.1 mM isopropyl-1-thio-β-D-galactopyranoside overnight. The cells were collected by centrifugation and frozen at -80 °C. For expression of seleno-methionine labelled GLRX5 the expression plasmid was transformed into *E.coli* strain B834(DE3) and cultures were grown at 25 °C in LB supplemented with 50 µg/mL kanamycin. The cells were grown until they reached an OD_{600} of 1.0, were washed three times with sterile water and resuspended in M9-minimal medium (Molecular Dimensions). The culture was used to inoculate M9-minimal media supplemented with 40 mg/L SeMet, 50 µg/mL kanamycin and 100 µM $FeCl_3$ and grown at 37 °C until they reached an OD_{600} of 0.8. The temperature was decreased to 18 °C and protein expression was induced with 0.5 mM isopropyl-1-thio-β-D-galactopyranoside overnight. The cells were harvested by centrifugation and stored at -80 °C. Cell pellets were resuspended in 50 mM HEPES, pH 7.5, 500 mM NaCl, 20 mM imidazole, 5 % glycerol, protease inhibitors (Complete, Sigma) and lysed by sonication. Cell debris and nucleic acids were removed by addition of 0.15 % (w/v) polyethyleneimine followed by centrifugation for 45 min at 40,000xg. The proteins were purified by nickel-affinity chromatography (5 ml Ni-sepharose FF, GE Healthcare) using a stepwise gradient of imidazole, and fractions were analysed by SDS-PAGE. The protein was concentrated and the buffer was exchanged to 50 mM HEPES, pH 7.5, 500 mM NaCl, 5 % (v/v) glycerol, 10 mM GSH, 3 mM dithiothreitol (DTT) and 0.5 mM tris(2-carboxyethyl)phosphine (TCEP) using an Amicon centrifugal filtration unit (Millipore, 3kDa MWCO). The histidine tag was removed by incubating GLRX5 with TEV protease (150 µg TEV/10 mg GLRX5) for 16 hours at 4 °C. The protein was re-purified by applying to a nickel affinity column (500 µl Ni-sepharose FF, GE Healthcare) and the flow-through was collected. The TEV-cleaved protein was concentrated using an Amicon 3K-centrifugal filtration unit and used for crystallisation and further characterisation.

Apo GLRX5 was obtained by addition of 5 mM EDTA followed by gel-filtration chromatography on a HiLoad 16/60 Superdex 200 column (GE Healthcare) equilibrated with a buffer composed of 10 mM HEPES pH 7.5, 500 mM NaCl, 5 % (v/v) glycerol, 5 mM GSH, 0.5 mM TCEP.

Spectroscopy

The concentration of GLRX5 was determined by measuring the absorbance at 280 nm using a Labtech, Nanodrop 1000 spectrophotometer and a predicted extinction coefficient of 11460 M^{-1} cm^{-1}. The stability of the FeS clusters was monitored aerobically at 20 °C for 240 min by measuring the absorbance at 320 and 420 nm using a polar star omega plate reader (BMG labtech) under varying conditions using 2-5 mM of GSH, GSSG, H_2O_2 or EDTA.

Molecular mass analysis

The molecular mass of GLRX5 was verified by electrospray ionization mass spectrometry (Agilient 1100 series LC/MSD).

Analytical gelfiltration chromatography

Apo and holo GLRX5 were applied to an analytical 10/300 Superdex 200 column (GE healthcare) equilibrated with 10 mM HEPES pH 7.5, 300 mM NaCl, 5 mM GSH, 0.5 mM TCEP at 4 ^{o}C. The column was calibrated with low molecular weight standards consisting of bovine albumin (66 kDa) and bovine carbonic anhydrase (29 kDa).

Analytical Ultracentrifugation

Sedimentation velocity experiments were carried out on a Beckman Optima XL-I Analytical Ultracentrifuge (Beckman Instruments, Palo Alto, CA) equipped with an AnTi-50 rotor and cells with double sector centerpieces. Protein samples were studied at a concentration of 50 µM in 10 mM HEPES pH 7.5, 300 mM NaCl at 10 ^{o}C, employing a rotor speed of 45,000 rpm. Radial absorbance scans were collected using absorbance optics at a wavelength of 280 nm in continuous scan mode, in 2 minute intervals with a radial step size of 0.003 cm. Aliquots (300 µL) were loaded into the sample chambers of double channel, 12 mm centerpieces and 310 µL of buffer was used in the reference channels. Data were analyzed using the SEDFIT [21] software package whereby differential sedimentation coefficient distributions, *c(s)* distributions, were obtained by direct boundary modeling to Lamm Equation solutions. Sedimentation coefficients, *s*, were obtained by integration of individual peaks in the calculated *c(s)* distributions, after fitting of the frictional ratio, in order to allow these distributions to be corrected for the effects of diffusion. The software package SEDNTERP [22] (version 1.08) was used in order to convert the obtained sedimentation coefficient values to the equivalent values in water at 20 °C, $s^0_{20,w}$, taking into account the solvent density (1.01313 g/mL), viscosity (1.567x10^{-2} poise), and partial specific volume (0.7255 or 0.7316 mL/g for the dimer or monomer.

Enzymatic characterisation of GLRX5

To measure GLRX activity, Di-Eosin-GSSG [23], was used to glutathionylate bovine serum albumin (BSA) (Montano, S J, Lu, J and Holmgren, A. manuscript in preparation). The Eosin-GSH-BSA was used as substrate and release of eosin-GSH, which is highly fluorescent with a 545 nm emission, was measured. A black 96-well plate was used in a Perkin Elmer Victor3 multi-label counter containing a final well volume of 100 µL with 1 µM apo GLRX5 or 10 nM GLRX2, 0.25 mM NADPH, 45 nM yeast glutathione reductase (GR) in 0.1 M potassium phosphate buffer pH 7.5, 1 mM EDTA and 20 µM of Eosin-GSH-BSA. The reaction was started by addition of 25, 50, 100, 200, 400 or 800 µM GSH followed by recording the fluorescence emission at 545 nm after 520 nm excitation. Controls where no GSH was added in the reactions were included in the experiment. In a separate experiment concentrations of 0, 0.5, 1, 2 and 4 µM GLRX5 or 0.625 to 20 nM GLRX2 were incubated with 0.5 mM GSH, 0.25 mM NADPH and 45 nM yeast GR in 0.1 M potassium phosphate buffer pH 7.5, 1 mM EDTA. The reaction was started by adding 20 µM of Eosin-GSH-BSA and the fluorescence was recorded. Controls in the absence of GLRX2/5 were included. In the final experiment, 60 nM rat recombinant full-length TXNRD1 [24], replaced GR and was incubated with up to 4 µM GLRX5 to test if this enzyme used GLRX5 as a substrate. The fluorescence increase per min at 545 nm was calculated within a linear range of the reaction curve to determine the catalytic activity of GLRX5 and GLRX2.

Ribonucleotide reductase (RNR) activity with GSH was used to test the activity of GLRX5. Proteins R1, R2 and p53R2 of RNR were expressed and purified as described before [25, 26]. Determination of RNR activities were carried out as described previously [25]. Briefly, RNR enzyme was reconstituted by mixing recombinant R1 and R2 or p53R2 proteins. Activity was assayed following the conversion of [^{3}H]CDP into [^{3}H]dCDP. R1 and R2 or p53R2 proteins were pre-incubated with 2 mM ATP and 10 mM $MgCl_2$ at 37 °C for 15 minutes and the reaction was initiated by adding reaction mixture containing 40 mM Tris-Cl buffer, pH 7.6, 2 mM ATP, 10 mM $MgCl_2$, 200 mM KCl, 20 µM $FeCl_3$, and 0.5 mM [^{3}H]CDP (~ 10,000 cpm/nmol) in a final volume of 50 µL. When a GLRX system was used together with RNR, the samples contained 2 µM of apo GLRX5, 0.15 µM GR, 1 mM NADPH, and 10 mM GSH. Incubation was carried out at 37 °C for 60 min. The reaction was terminated by the addition of 1 M $HClO_4$, which also hydrolyzes dCDP to dCMP. The amount of [^{3}H]dCMP radioactivity was quantified by liquid scintillation counting after ion exchange chromatography on Dowex-50 columns. The activity

was calculated as nmol of dCDP produced (measured as dCMP) per time of incubation and OriginPro 8.1 software used for data analysis.

Crystallisation

SeMet substituted crystals were grown by vapor diffusion employing the sitting drop method, using 75 nL protein (37 mg/mL) and 75 nL well solution containing 70 % (v/v) 2-methyl-2,4-pentanediol (MPD) and 0.1 M HEPES pH 7.5. Native crystals were grown using the same technique in a drop of 150 nL protein (93 mg/mL) and 150 nL well solution containing 50 % (v/v) PEG300, 0.2 M $MgCl_2$, 0.1 M cacodylate pH 6.5 and 0.01 M spermine tetrahydrochloride. Both types of crystals were grown aerobically at 20 ºC, were shaped like thin rods and were visibly brown. The crystals were flash cooled in liquid nitrogen straight from the drop without additional cryo-protection.

X-ray data collection and refinement

Both the SeMet and the high resolution X-ray data were collected at 100 K on beam line X10SA at the Swiss Light Source. The SeMet crystal diffracted to 2.7 Å and was collected at the wavelength λ=0.9794 Å. After processing in Mosflm [27] the data were analyzed in XPREP (Bruker AXS) and 4 SeMet sites were found using SHELXD [28] with an anomalous signal to 3.1 Å. Initial phases were calculated with SHELXE and the space group pinpointed to $P4_32_12$. The phases were improved in SHARP [29] and Buccaneer [30] was used to build fragments of secondary structural elements into the solvent-flattened maps. Positions for four molecules of the closest homolog, GLRX C1 from *Populus tremula x tremuloides* (PDB ID 2E7P), were found by manual molecular replacement in Coot [31] using the Buccaneer built fragments as a guide. After rigid body refinement in REFMAC5 [32] and phase improvement using Parrot [33] the maps enabled a first rough rebuild in Coot. The resulting model was used for molecular replacement into the higher resolution native data with Phaser [34]. The native data were collected at λ=0.979Å in 5 wedges along the thin, rod-like native crystal that showed highly anisotropic diffraction. In each segment, 20 degrees of data survived radiation damage. The frames were integrated with Mosflm and data were merged and scaled using Scala from CCP4 suite to a final resolution of 2.4 Å [27]. Before refinement commenced, 5% of the data were set aside for the calculation of R_{free}. The maps from the Phaser solution were automatically traced by ARP/wARP [35] and the model was improved by manual rebuilding in Coot cycled with restrained refinement in REFMAC5 including translation/liberation/screw (TLS) groups. Refinement included all data to 2.4 Å although due to the anisotropy of the data the final resolution of the structure is considered to be 2.6 Å. The final model and structure factors have been deposited in the PDB with the accession code 2WUL. Statistics are presented in supplemental table 1.

Electrostatic surface potential

The PDB2PQR server [36] was used to convert the protein files to PQR format and charges were assigned using the PARSE force field. The Adaptive Poisson-Boltzmann Solver (APBS) plugin for PyMOL was used to map the electrostatic potential (± 5 kT/e) onto the molecular surface of the protein.

RESULTS

Purification and analysis by UV-VIS spectroscopy. On the basis of previous experience with human GLRX2, holo GLRX5 was purified aerobically in the presence of reduced GSH and TCEP. Holo GLRX5 had a visible brown color and absorbed light of 320, 415, 420 and 457 nm wavelength, characteristic of a [2Fe2S] centre [1] whereas the apo protein had no absorption in this region (supplemental figure 1). The stability of the clusters in holo GLRX5 and holo GLRX2 was followed at 420 nm after addition of GSH, EDTA, GSSG, or H_2O_2 (figure 1). GLRX5 precipitated immediately when 2 mM GSSG was added to the holo enzyme (data not shown) and

75 min after addition of 5 mM H_2O_2. This is in contrast to holo GLRX2 where both GSSG and H_2O_2 slowly destabilizes the cluster but does not precipitate the protein. Addition of EDTA affected cluster dissociation faster in holo GLRX5 compared to holo GLRX2 whereas GSH seemed to stabilise the cluster in both proteins. These results reveal differences in cluster stability and interaction with redox compounds.

Analysis of the oligomeric state. In gelfiltration chromatography experiments holo and apo GLRX5 eluted as two peaks corresponding to apparent molecular weights of 52 kDa (tetramer) and 13 kDa (monomer) (figure 2A). This is in contrast to holo GLRX2, which is a dimer in solution. The tetrameric quaternary state of holo GLRX5 was further supported by sedimentation velocity analytical ultracentrifugation that confirmed that holo GLRX5 is a tetramer in solution whereas apo GLRX5 is monomeric (figure 2b). Hence, tetramerization of GLRX5 is coupled to iron-sulphur cluster binding.

Molecular mass analysis. The molecular mass of native and SeMet labeled holo GLRX5 was determined to 12852 and 12946 Da, respectively, in agreement with the predicted mass of the expressed constructs. Analysis of apo GLRX5 identified three peaks of 13464, 13158 and12851 Da (figure 3). The masses of the first two peaks are consistent with the addition of two and one GSH molecule, respectively, whereas the third peak potentially could corresponds to an intra-molecular disulfide. Tryptic digestion of the apo protein followed by Ion-trap mass spectrometry (MS-MS) analysis identified only glutathionylation of Cys67 and no other cysteine containing fragment corresponding to glutathionylation of Cys122 or an intramolecular disulfide was detected (data not shown).

Crystal structure of [2Fe2S]-bound GLRX5. The crystallographic asymmetric unit contains 436 protein residues in four chains (A_{41-149}, B_{41-149}, C_{40-148}, and D_{41-149}), four GSH molecules, two inorganic [2Fe2S] clusters, four chloride ions, one molecule of polyethylene glycol, and 93 water molecules. In addition, the electron density map reveals an unknown entity in close proximity to Phe69 and GSH in each molecule that was left unmodelled. More than 99 % of residues are in favoured regions and all are in allowed regions of a Ramachandran plot calculated by MolProbity [37].

The [2Fe2S] clusters are each coordinated by two protein chains and two GSH molecules where the iron atoms are tetrahedrally coordinated by active site Cys67, a cysteine contributed by GSH and two inorganic sulphurs. In this way there are two [2Fe2S] coordinated dimers whereby ~1050 $Å^2$ surface area of the two protein chains are buried upon dimer formation. Analysis of the crystal packing suggests a tetrameric form (figure 4A) with an additional 840 $Å^2$ of surface area buried upon tetramer formation. The cluster is completely buried from the exterior and solvent accessibility is only possible via the central aperture. The GSH molecules and the position of the Phe69 side-chain further reduce the solvent accessibility of the cluster (figure 4C). Each protein chain comprises a central four-stranded mixed beta sheet flanked by five alpha helices typical of the thioredoxin superfamily of proteins. Cys67 is located at the N-terminus of helix α2 and the loop between beta strand β1 and helix α2 (β1-α2 loop, residues 59-67) forms a β-hairpin which is folded back onto the protomer and packs against α2 and β2.

Lys59, which is conserved in both monothiol and dithiol GLRXs, anchors the beginning of the β1-α2 loop whereby the backbone NH forms a hydrogen bond with the hydroxyl of Ser70 (2.8-3.0 Å, in the four protein chains) whereas the backbone carbonyl forms a hydrogen bond to the backbone NH in Gln66 (3.0 Å). The Lys59 side-chain has two ionic interactions with the GSH that is closely associated with the protein chain: one with the glycine carboxylate (2.5-2.7 Å) and another with the cysteine thiolate (3.0-3.4 Å). NZ of Lys59 also forms a hydrogen bond with the backbone carbonyl of Gln66 (2.6-2.9 Å) from the associated protein molecule that coordinates the cluster. The β1-α2 loop is further stabilised by hydrogen bonds between the backbone NH of Thr61 and the backbone carbonyl in Gln64 and between the hydroxyl of Thr61 and the backbone

NH of Gln64 (3.0 Å). Finally, the Cys67 anchors the C-terminus of the β1-α2 loop and its role in coordinating the [2Fe2S] cluster. The charged side chains of Glu63 and Gln64 in the β1-α2 loop, as well as Asp92 and Asp93 in the β2-α3 loop, stretch out away from the protein.
The only other cysteine present in the protein sequence, Cys122, is located in the beginning of helix α4. Cys122 is separated from Cys67 by 7.6-8.4 Å (sulphur to sulphur distance) and the side chain of Phe69 intercalates between the two cysteine side chains.
The interface between the two molecules that coordinate the cluster is not completely symmetrical: Arg97 interacts across the interface by forming intermolecular hydrogen bonds with the main-chain carbonyl of Pro65 (Arg97A-Pro65B, Arg97C-Pro65D) or the Gln66 side-chain (Arg97B-Gln66A, Arg97D-Gln66C). Two residues, Trp106 and Pro107, located on α3-β3 loop stabilize the tetramer by packing against the α4 helix in the neighbouring subunit (A-D and B-C).

Each of the GSH molecules that coordinate the [2Fe2S] cluster makes extensive contacts with an individual protein chain (figure 4B). The Glu carboxylate accepts hydrogen bonds from the backbone nitrogens of Cys122 and Asp123 and the Glu amine participates in a salt bridge with the side chain of Asp123. The GSH Cys has two backbone interactions with the main chain of Ile109 and the glycine carboxylate has ionic interactions with the side chains of Lys59, Arg97 and Lys101.

Analysis of the surface charge. Analysis of the sequence of GLRX5 reveals that it is an acidic protein with a predicted iso-electric point of 4.5. This is in contradiction to GLRX2 which has a predicted iso-electric point of 9.2. Mapping the electrostatic potential onto the surface of the proteins as shown in figure 5 illustrates the difference in the surface properties of the two proteins. The results suggest that GLRX5 and GLRX2 likely have different interaction partners or possibly even interact with each other.

Enzymatic activity. Since one of the most obvious roles for GLRXs in FeS cluster assembly or transfer is to reduce disulfides or mixed disulfides with GSH on FeS acceptor proteins we measured whether GLRX5 could reduce mixed disulfides with GSH. When GSH was used as an electron donor, micromolar concentrations of GLRX5 catalyzed the reduction of glutathionylated BSA (figure 6A). This can be compared with human GLRX2 that under the same conditions reduced glutathionylated BSA in nanomolar concentrations (figure 6B). These results show that the relative catalytic activity of GLRX5 is approximately 500 times lower than GLRX2. No activity was detected when TXNRD1 was used as an electron donor instead of GSH. Thus, unlike GLRX2 [38], GLRX5 is not a direct substrate of TXNRD1 (data not shown). To study the reduction of the GLRX-glutathione intermediate, potentially formed in the second step in the reaction above [39, 40], 20 μM Eosin-GSH-BSA was used with either 1 μM GLRX5 or 10 nM GLRX2 and the GSH concentration varied (figure 6C and 6D). These results reveal that the GSH-GLRX5 mixed disulfide is reduced with a rate at least 100 times slower than that of GSH-GLRX2 (table 1).
To test if GLRX5 was acting as an electron donor for RNR, experiments were performed with different concentrations of GSH in combination with human GLRX5 and mouse R1-R2 complex. With 5 mM GSH, no RNR activity was recorded with GLRX5 system; while 10 and 20 mM GSH showed significant activity for RNR catalysis (figure 7A). RNR activity was also recorded for the R1-R2 complex with varying concentrations of human GLRX5 (0.1–5 μM) in the presence of 10 mM GSH, 1 mM NADPH, and 0.15 μM GR (figure 7 B). A K_m value of 0.4 μM was obtained for GLRX5 with R1-R2 complex. The same experiment was performed with the R1-p53R2 complex and it displayed a typical apparent K_m value of 0.9 μM for GLRX5 (figure 7B).

DISCUSSION

After analysis of the GLRX5 crystal structure revealed a tetrameric organisation, studies to determine the quaternary structure in solution were initiated. Analytical ultra-centrifugation and size-exclusion chromatography support that holo GLRX5 is tetrameric while the metal-free protein is monomeric. Thus far, only the monothiol GLRX6 from *Saccharomyces cerevisiae* is reported to be a tetramer in solution when coordinating a FeS-cluster [10]. A recently described structure of GLRX6 is of the FeS-free GSH-bound monomeric form while the tetrameric form apparently requires both FeS and an N-terminal domain [41]. Analysis of the crystal packing of the *E. coli* GLRX4 (a homolog to human GLRX5), using the Protein interfaces, surfaces and assemblies service (PISA) at the European Bioinformatics Institute also supports a tetrameric quaternary structure for GLRX4. Although the [2Fe2S]-bound dithiol poplar GLRX C1 (GRXC1) crystallises with a tetramer in the asymmetric unit, only two chains coordinate a [2Fe2S] cluster while the other two chains are apo proteins. Consequently it was shown that the tetrameric form of GRXC1 is a result of crystal packing since the protein is dimeric in solution. Thus the apparent oligomeric structure for the [2Fe2S]-bound monothiol GLRXs (GLRX4 and GLRX5), is different than the dimeric structure observed for the [2Fe2S]-bound dithiol GLRXs (GLRX2 and GRXC1). Compared to the GLRX2 dimer, the two protein chains that coordinate the [2Fe2S] cluster in GLRX5 are in a more extended conformation. The two GLRX5 protomers bind the cluster in a head-to-head fashion in which the two beta sheets are essentially co-planar. However, in GLRX2 the protomers that coordinate the [2Fe2S] cluster are organized such that the beta sheets form a ~120 degree angle and one is rotated by about 90°. The extended arrangement seen in GLRX5 was also observed for *E. coli* GLRX4 [42] and could be necessary to support tetramerisation since the bent conformation observed for the GLRX2 dimer would sterically interfere with this type of tetramer oligomerisation.

The inter-subunit interactions in GLRX5 are more extensive than those observed in human GLRX2 and are found between Lys59, Pro65, Gln66, and Arg97. Interestingly Lys59, Pro65 and Arg97 are conserved in monothiol GLRXs and Lys59, Pro65 and Gln66 are located on the extended β1-α2 loop that in the tetrameric structure shields the [2Fe2S] cluster. The position of the β1-α2 loop is similar in the *E. coli* GLRX4 [2Fe2S]-bound structure [42] while in the solution structure of monomeric *E. coli* GLRX4 [43] the loop protrudes away from the protein. Structural alterations of this loop have previously been suggested to be involved in cluster transfer [42] since it affects the position of Cys67 and contains several residues that both interact with GSH and are involved in protomer interactions. In holo GLRX5, the clusters are buried in the tetrameric structure and largely inaccessible. However, if the proteins implicated in cluster transfer were to interact with the β1-α2 loop and potentially also the β2-α3 loop in protomer A and B or C and D, they would gain close proximity to the cluster. In the current structure the conformation of the loops are stabilized by several hydrogen bonds and charged residues in both the β1-α2 loop (Glu63, Gln64) and the β2-α3 loop (Asp92, Asp93), which is conserved among most monothiol GLRXs, reach out into the solution. Thus, it would be interesting to do mutational studies of these residues once the interaction partners of GLRX5 are known.

Besides the cysteine in the CGFS active site motif GLRX5 possess a second, semi-conserved cysteine Cys122, that in yeast has been shown to form an intra-molecular disulfide with Cys67 [44, 45]. We have not been able to find conclusive evidence of such disulfide, that would require structural rearrangements including unwinding of the first turn of helix α2. This would not be unprecedented as a similar type of disulfide and helix unwinding has been observed upon oxidation of both human GLRX1 and human TXN1 [46, 47]. Thus, the proved sensitivity of apo and holo GLRX5 to GSSG or H_2O_2 might be due to destabilising structural rearrangements, possibly by formation of such an intra-molecular disulfide. The higher reactivity towards GSSG

compared to H_2O_2, is potentially due to the glutathione binding site or that GSH in the cluster might exchange with the GSH in the buffer, similar to holo GLRX2[48].

Mass spectrometry analysis revealed that GLRX5 *in vitro* can be covalently modified by one and two GSH molecules if the [2Fe2S] cluster is not present. Although we were only able to identify a GSH-mixed disulfide with Cys67, the most plausible explanation is that both Cys67 and Cys122 are modified by GSH. In the current structure of GLRX5, Cys67 is located ~3.8 Å from the GSH cysteine thiol and could readily form a mixed disulfide without significant rearrangement if the [2Fe2S] cluster was not present. GSH bound non-covalently to *S. cerevisiae* GLRX6 [41] adopts a similar binding mode as it does when covalently attached in GSH-GLRX mixed disulfides [6] and in human GLRX2 the non-covalently bound GSH also makes similar interactions with the protein as it does when coordinating the [2Fe2S] cluster [6]. Thus, glutathionylation of GLRX5 would protect the cysteine thiols from further oxidation and potentially also facilitate transfer or acceptance of the clusters.

Both glutathionylated BSA and RNR revealed that apo GLRX5 has low but significant deglutathionylation activity. In the reduction of glutathionylated BSA, the second half reaction is a 100-fold slower than that measured for GLRX2 and this result is similar to most monothiol GLRXs [9, 44, 49]. Reduction of the GLRX-GSH mixed disulfide by GSH might be inhibited by the five amino-acid insertion on the β1-α2 loop, or could be disfavoured if the GLRX-GSH mixed disulfide serves as a scaffold for FeS clusters [50]. GLRX5 also reduced the R1-R2 complex with a K_m which is comparable to previous studies with TXN1 and GLRX1 [25]. However, the specific activity and apparent V_{max} with RNR with R2 or p53R2 were found to be much lower for GLRX5 compared to GLRX1 or GLRX2[25]. Thus, the activity of both of the RNR complexes with GLRX5 reconfirms the glutathionylation mechanism for GLRX catalysis in contrast to the dithiol mechanism for TXN. Although the results clearly show that GLRX5 is active, its *in vivo* role in ribonucleotide reduction may be limited.

FUNDING

Supported by grants from Swedish Research Council, Swedish Cancer Society and The K.A Wallenberg Foundation. RS was supported by a Wenner-Gren postdoctoral fellowship. The Structural Genomics Consortium is a registered charity (Number 1097737) funded by the Canadian Institutes for Health Research, the Canadian Foundation for Innovation, Genome Canada through the Ontario Genomics Institute, GlaxoSmithKline, Karolinska Institutet, the Knut and Alice Wallenberg Foundation, the Ontario Innovation Trust, the Ontario Ministry for Research and Innovation, Merck and Co., Inc., the Novartis Research Foundation, the Swedish Agency for Innovation Systems, the Swedish Foundation for Strategic Research and the Wellcome Trust. The study was supported by the Oxford NIHR Biomedical Research Unit.

REFERENCES

1 Lillig, C. H., Berndt, C., Vergnolle, O., Lonn, M. E., Hudemann, C., Bill, E. and Holmgren, A. (2005) Characterization of human glutaredoxin 2 as iron-sulfur protein: a possible role as redox sensor. Proc Natl Acad Sci U S A. **102**, 8168-8173

2 Rouhier, N., Unno, H., Bandyopadhyay, S., Masip, L., Kim, S. K., Hirasawa, M., Gualberto, J. M., Lattard, V., Kusunoki, M., Knaff, D. B., Georgiou, G., Hase, T., Johnson, M. K. and Jacquot, J. P. (2007) Functional, structural, and spectroscopic characterization of a glutathione-ligated [2Fe-2S] cluster in poplar glutaredoxin C1. Proc Natl Acad Sci U S A. **104**, 7379-7384

3 Tripathi, T., Rahlfs, S., Becker, K. and Bhakuni, V. (2008) Structural and stability characteristics of a monothiol glutaredoxin: glutaredoxin-like protein 1 from Plasmodium falciparum. Biochim Biophys Acta. **1784**, 946-952

4 Picciocchi, A., Saguez, C., Boussac, A., Cassier-Chauvat, C. and Chauvat, F. (2007) CGFS-type monothiol glutaredoxins from the cyanobacterium Synechocystis PCC6803 and other evolutionary distant model organisms possess a glutathione-ligated [2Fe-2S] cluster. Biochemistry. **46**, 15018-15026

5 Comini, M. A., Rettig, J., Dirdjaja, N., Hanschmann, E. M., Berndt, C. and Krauth-Siegel, R. L. (2008) Monothiol glutaredoxin-1 is an essential iron-sulfur protein in the mitochondrion of African trypanosomes. J Biol Chem. **283**, 27785-27798

6 Johansson, C., Kavanagh, K. L., Gileadi, O. and Oppermann, U. (2007) Reversible sequestration of active site cysteines in a 2Fe-2S-bridged dimer provides a mechanism for glutaredoxin 2 regulation in human mitochondria. J Biol Chem. **282**, 3077-3082

7 Lillig, C. H., Berndt, C. and Holmgren, A. (2008) Glutaredoxin systems. Biochim Biophys Acta. **1780**, 1304-1317

8 Belli, G., Polaina, J., Tamarit, J., De La Torre, M. A., Rodriguez-Manzaneque, M. T., Ros, J. and Herrero, E. (2002) Structure-function analysis of yeast Grx5 monothiol glutaredoxin defines essential amino acids for the function of the protein. J Biol Chem. **277**, 37590-37596

9 Fernandes, A. P., Fladvad, M., Berndt, C., Andresen, C., Lillig, C. H., Neubauer, P., Sunnerhagen, M., Holmgren, A. and Vlamis-Gardikas, A. (2005) A novel monothiol glutaredoxin (Grx4) from Escherichia coli can serve as a substrate for thioredoxin reductase. J Biol Chem. **280**, 24544-24552

10 Mesecke, N., Mittler, S., Eckers, E., Herrmann, J. M. and Deponte, M. (2008) Two novel monothiol glutaredoxins from Saccharomyces cerevisiae provide further insight into iron-sulfur cluster binding, oligomerization, and enzymatic activity of glutaredoxins. Biochemistry. **47**, 1452-1463

11 Rodriguez-Manzaneque, M. T., Tamarit, J., Belli, G., Ros, J. and Herrero, E. (2002) Grx5 is a mitochondrial glutaredoxin required for the activity of iron/sulfur enzymes. Mol Biol Cell. **13**, 1109-1121

12 Ojeda, L., Keller, G., Muhlenhoff, U., Rutherford, J. C., Lill, R. and Winge, D. R. (2006) Role of Glutaredoxin-3 and Glutaredoxin-4 in the Iron Regulation of the Aft1 Transcriptional Activator in Saccharomyces cerevisiae. J Biol Chem. **281**, 17661-17669

13 Molina-Navarro, M. M., Casas, C., Piedrafita, L., Belli, G. and Herrero, E. (2006) Prokaryotic and eukaryotic monothiol glutaredoxins are able to perform the functions of Grx5 in the biogenesis of Fe/S clusters in yeast mitochondria. FEBS Lett. **580**, 2273-2280

14 Ye, H., Jeong, S. Y., Ghosh, M. C., Kovtunovych, G., Silvestri, L., Ortillo, D., Uchida, N., Tisdale, J., Camaschella, C. and Rouault, T. A. (2010) Glutaredoxin 5 deficiency causes sideroblastic anemia by specifically impairing heme biosynthesis and depleting cytosolic iron in human erythroblasts. J Clin Invest. **120**, 1749-1761
15 Wingert, R. A., Galloway, J. L., Barut, B., Foott, H., Fraenkel, P., Axe, J. L., Weber, G. J., Dooley, K., Davidson, A. J., Schmid, B., Paw, B. H., Shaw, G. C., Kingsley, P., Palis, J., Schubert, H., Chen, O., Kaplan, J. and Zon, L. I. (2005) Deficiency of glutaredoxin 5 reveals Fe-S clusters are required for vertebrate haem synthesis. Nature. **436**, 1035-1039
16 Witte, S., Villalba, M., Bi, K., Liu, Y., Isakov, N. and Altman, A. (2000) Inhibition of the c-Jun N-terminal kinase/AP-1 and NF-kappaB pathways by PICOT, a novel protein kinase C-interacting protein with a thioredoxin homology domain. J Biol Chem. **275**, 1902-1909
17 Rundlof, A. K., Janard, M., Miranda-Vizuete, A. and Arner, E. S. (2004) Evidence for intriguingly complex transcription of human thioredoxin reductase 1. Free Radic Biol Med. **36**, 641-656
18 Vilella, F., Alves, R., Rodriguez-Manzaneque, M. T., Belli, G., Swaminathan, S., Sunnerhagen, P. and Herrero, E. (2004) Evolution and cellular function of monothiol glutaredoxins: involvement in iron-sulphur cluster assembly. Comp Funct Genomics. **5**, 328-341
19 Muhlenhoff, U., Gerber, J., Richhardt, N. and Lill, R. (2003) Components involved in assembly and dislocation of iron-sulfur clusters on the scaffold protein Isu1p. EMBO J. **22**, 4815-4825
20 Camaschella, C., Campanella, A., De Falco, L., Boschetto, L., Merlini, R., Silvestri, L., Levi, S. and Iolascon, A. (2007) The human counterpart of zebrafish shiraz shows sideroblastic-like microcytic anemia and iron overload. Blood. **110**, 1353-1358
21 Schuck, P. (2000) Size-distribution analysis of macromolecules by sedimentation velocity ultracentrifugation and lamm equation modeling. Biophys J. **78**, 1606-1619
22 Laue, T. M. (1992) *Analytical ultracentrifugation in biochemistry and polymer science Analytical ultracentrifugation in biochemistry and polymer science* Royal Society of Chemistry, 90-125
23 Raturi, A. and Mutus, B. (2007) Characterization of redox state and reductase activity of protein disulfide isomerase under different redox environments using a sensitive fluorescent assay. Free Radic Biol Med. **43**, 62-70
24 Rengby, O., Cheng, Q., Vahter, M., Jornvall, H. and Arner, E. S. (2009) Highly active dimeric and low-activity tetrameric forms of selenium-containing rat thioredoxin reductase 1. Free Radic Biol Med. **46**, 893-904
25 Avval, F. Z. and Holmgren, A. (2009) Molecular mechanisms of thioredoxin and glutaredoxin as hydrogen donors for Mammalian s phase ribonucleotide reductase. J Biol Chem. **284**, 8233-8240
26 Guittet, O., Hakansson, P., Voevodskaya, N., Fridd, S., Graslund, A., Arakawa, H., Nakamura, Y. and Thelander, L. (2001) Mammalian p53R2 protein forms an active ribonucleotide reductase in vitro with the R1 protein, which is expressed both in resting cells in response to DNA damage and in proliferating cells. J Biol Chem. **276**, 40647-40651

27 CCP4. (1994) The CCP4 suite: programs for protein crystallography. Acta Crystallogr D Biol Crystallogr. **50**, 760-763
28 Sheldrick, G. M. (2008) A short history of SHELX. Acta Crystallogr A. **64**, 112-122
29 Fortelle, E. d. l. B., G. (1997) Maximum-likelihood heavy-atom parameter refinement for multiple isomorphous replacement and multiwavelength anomalous diffraction methods. Methods in Enzymology. **276**, 472-494
30 Cowtan, K. (2006) The Buccaneer software for automated model building. 1. Tracing protein chains. Acta Crystallogr D Biol Crystallogr. **62**, 1002-1011
31 Emsley, P. and Cowtan, K. (2004) Coot: model-building tools for molecular graphics. Acta Crystallogr D Biol Crystallogr. **60**, 2126-2132
32 Murshudov, G. N., Vagin, A. A. and Dodson, E. J. (1997) Refinement of macromolecular structures by the maximum-likelihood method. Acta Crystallogr D Biol Crystallogr. **53**, 240-255
33 Zhang, K. Y., Cowtan, K. and Main, P. (1997) Combining constraints for electron-density modification. Methods Enzymol. **277**, 53-64
34 McCoy, A. J., Grosse-Kunstleve, R. W., Storoni, L. C. and Read, R. J. (2005) Likelihood-enhanced fast translation functions. Acta Crystallogr D Biol Crystallogr. **61**, 458-464
35 Perrakis, A., Harkiolaki, M., Wilson, K. S. and Lamzin, V. S. (2001) ARP/wARP and molecular replacement. Acta Crystallogr D Biol Crystallogr. **57**, 1445-1450
36 Dolinsky, T. J., Czodrowski, P., Li, H., Nielsen, J. E., Jensen, J. H., Klebe, G. and Baker, N. A. (2007) PDB2PQR: expanding and upgrading automated preparation of biomolecular structures for molecular simulations. Nucleic Acids Res. **35**, W522-525
37 Chen, V. B., Arendall, W. B., 3rd, Headd, J. J., Keedy, D. A., Immormino, R. M., Kapral, G. J., Murray, L. W., Richardson, J. S. and Richardson, D. C. MolProbity: all-atom structure validation for macromolecular crystallography. Acta Crystallogr D Biol Crystallogr. **66**, 12-21
38 Johansson, C., Lillig, C. H. and Holmgren, A. (2004) Human mitochondrial glutaredoxin reduces s-glutathionylated proteins with high affinity accepting electrons from either glutathione or thioredoxin reductase. J Biol Chem. **279**, 7537-7543.
39 Holmgren, A. and Åslund, F. (1995) Glutaredoxin. Methods Enzymol. **252**, 283-292
40 Gravina, S. A. and Mieyal, J. J. (1993) Thioltransferase is a specific glutathionyl mixed disulfide oxidoreductase. Biochemistry. **32**, 3368-3376
41 Luo, M., Jiang, Y. L., Ma, X. X., Tang, Y. J., He, Y. X., Yu, J., Zhang, R. G., Chen, Y. and Zhou, C. Z. (2010) Structural and biochemical characterization of yeast monothiol glutaredoxin Grx6. J Mol Biol. **398**, 614-622
42 Iwema, T., Picciocchi, A., Traore, D. A., Ferrer, J. L., Chauvat, F. and Jacquamet, L. (2009) Structural basis for delivery of the intact [Fe2S2] cluster by monothiol glutaredoxin. Biochemistry. **48**, 6041-6043
43 Fladvad, M., Bellanda, M., Fernandes, A. P., Mammi, S., Vlamis-Gardikas, A., Holmgren, A. and Sunnerhagen, M. (2005) Molecular mapping of functionalities in the solution structure of reduced Grx4, a monothiol glutaredoxin from Escherichia coli. J Biol Chem. **280**, 24553-24561

44 Tamarit, J., Belli, G., Cabiscol, E., Herrero, E. and Ros, J. (2003) Biochemical characterization of yeast mitochondrial Grx5 monothiol glutaredoxin. J Biol Chem. **278**, 25745-25751

45 Zaffagnini, M., Michelet, L., Massot, V., Trost, P. and Lemaire, S. D. (2008) Biochemical characterization of glutaredoxins from Chlamydomonas reinhardtii reveals the unique properties of a chloroplastic CGFS-type glutaredoxin. J Biol Chem. **283**, 8868-8876

46 Hashemy, S. I., Johansson, C., Berndt, C., Lillig, C. H. and Holmgren, A. (2007) Oxidation and S-nitrosylation of cysteines in human cytosolic and mitochondrial glutaredoxins: effects on structure and activity. J Biol Chem. **282**, 14428-14436

47 Watson, W. H., Pohl, J., Montfort, W. R., Stuchlik, O., Reed, M. S., Powis, G. and Jones, D. P. (2003) Redox potential of human thioredoxin 1 and identification of a second dithiol/disulfide motif. J Biol Chem. **278**, 33408-33415

48 Berndt, C., Hudemann, C., Hanschmann, E. M., Axelsson, R., Holmgren, A. and Lillig, C. H. (2007) How does iron-sulfur cluster coordination regulate the activity of human glutaredoxin 2? Antioxid Redox Signal. **9**, 151-157

49 Rahlfs, S., Fischer, M. and Becker, K. (2001) Plasmodium falciparum possesses a classical glutaredoxin and a second, glutaredoxin-like protein with a PICOT homology domain. J Biol Chem. **276**, 37133-37140

50 Eckers, E., Bien, M., Stroobant, V., Herrmann, J. M. and Deponte, M. (2009) Biochemical characterization of dithiol glutaredoxin 8 from Saccharomyces cerevisiae: the catalytic redox mechanism redux. Biochemistry. **48**, 1410-1423

.

FIGURE LEGENDS

FIGURE 1: Stability of the iron-sulphur cluster in GLRX5 in comparison to GLRX2. The stability of the [2Fe2S] cluster in GLRX2 (A) and GLRX5 (B) was monitored aerobically by measuring the absorbance at 420 nm at 20 ºC for 240 min using a polar star omega plate reader after addition of 2 mM of either GSH, H_2O_2 or EDTA, and the absorbance corrected to the protein concentration used. *Grey line, untreated protein. Black line, GSH. Dashed lines, H_2O_2. Open circles, EDTA.*

FIGURE 2: The oligomeric state of apo- and holo GLRX5 analysed by gelfiltration chromatography and by sedimentation velocity analytical ultracentrifugation.
A. Apo (dotted line) and holo GLRX5 (black line) were applied onto a Superdex 200 column equilibrated with 10 mM HEPES pH 7.5, 300 mM NaCl, 5 mM GSH, 0.5 mM TCEP at 4 ºC. The column was calibrated with low molecular weight standards (grey filled area) consisting of bovine albumin (66 kDa) and bovine carbonic anhydrase (29 kDa). B. Sedimentation velocity plot of the differential sedimentation coefficient distribution, *c(s)*, versus the apparent sedimentation coefficient corrected to water at 20 ^{o}C, $s_{20,w}$ of GLRX5, together with the differential molecular weight distribution, *c(M)*, versus the system mass, *M*. Experiments were conducted with a protein concentration of 13 µM in 10 mM HEPES, pH 7.5, 300 mM NaCl at 4 ^{o}C. The protein sediments as a monomer (dotted line) in the absence of an [2Fe2S] cluster, or as a mixture of monomer and tetramer (black line) in the presence of an [2Fe2S] cluster.

FIGURE 3: Molecular mass of apo GLRX5. The molecular weight of apo GLRX5 was verified by electrospray mass ionization-time-of-flight mass spectrometry.

FIGURE4: **Structure of human GLRX5**. A. Tetramer colored by protein chain with the β1-α2 loop shown in crimson. The [2Fe2S] cluster is represented by orange and yellow spheres (for iron and sulfur, respectively) while the GSH is shown as sticks with carbon colored white, nitrogen blue, and oxygen red. Phe69 which shields the cluster from solvent is also shown in stick representation with carbons colored by protein chain. B. Interactions between GSH and the protein chains where main-chain contacts are depicted by black triangles and hydrogen bonds are shown by dashed lines. C. Stereo view of [2Fe2S] cluster coordination and intersubunit interactions. View is looking at the tetramer edge as shown by the arrow and icon in panel A. [2Fe2S]-cluster coordination and intersubunit interactions are shown by black and yellow dotted lines respectively. Features associated with protein chain B are marked by an asterisk.

FIGURE 5: Electrostatic potential (± 5 kT/e) mapped onto the molecular surface.
A. GLRX5 tetramer. B. GLRX2 dimer.

FIGURE 6: Characterisation of GLRX5 and comparison to GLRX2 as GSH-disulfide oxidoreductases.
In 100 µL 0.25 mM NADPH, 0.5 mM GSH and 45 nM yeast GR were incubated with 0 to 4 µM GLRX5 (A) or 0 to20 nM GLRX2 (B). Subsequently, GSH concentrations of 25-800 µM were added to 1 µM GLRX5 (C) or 10 nM GLRX2 (D) in the presence of 0.25 mM NADPH and 45 nM yeast GR. Reactions were started by addition of 20 µM Eosin-GSH-BSA and the relative fluorescence recorded at 545 nm. Hanes-Woolf plots are shown in insets and the OriginPro 8.1 software used for data analysis

FIGURE 7: Effect of GLRX5 and GSH on mouse RNR complexes in reduction of CDP to dCDP. A. Samples with 200 µg/mL of R1 and 40 µg/mL R2 were assayed with varying

concentrations of GSH. The reaction was started by adding reaction mixture supplemented with 2 μM GLRX5, 1 mM NADPH, and 0.15 μM yeast GR.
B. RNR activity of 200 μg/mL R1 with 100 μg/mL R2 (closed circles) or 100 μg/mL p53R2 (open triangles) were measured in the presence of increasing amounts of GLRX5 with 1 mM NADPH, 10 mM GSH, and 0.15 μM yeast GR. The results represent two independent experiments with duplicate samples. The kinetic data was determined from a double reciprocal Lineweaver Burke plot using the OriginPro 8.1 software.

Biochemical Journal Immediate Publication. Published on 29 Oct 2010 as manuscript BJ20101286

TABLE 1. Kinetic constants for GSH-dependent reduction of mixed disulfides

Protein	GSH		
	K_m (μM)	k_{cat} (s^{-1})	k_{cat}/K_m ($M^{-1}\cdot s^{-1}$)
GLRX2	238	398	1.7×10^6
GLRX5	233	4.3	1.8×10^4

FIGURE 1.

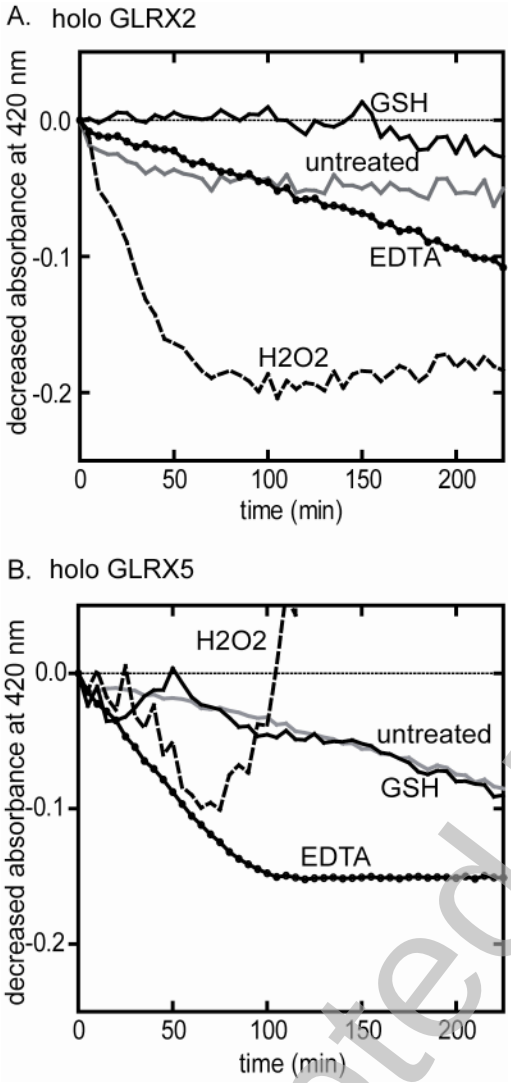

FIGURE 2.

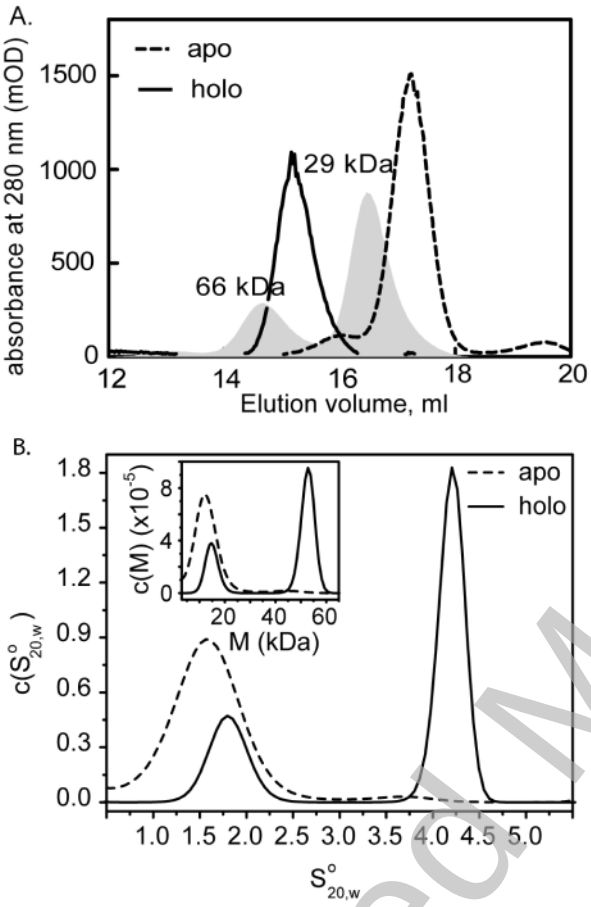

FIGURE 3.

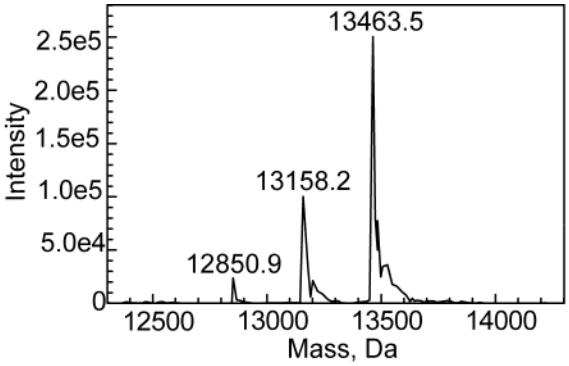

Biochemical Journal Immediate Publication. Published on 29 Oct 2010 as manuscript BJ20101286

FIGURE 4.

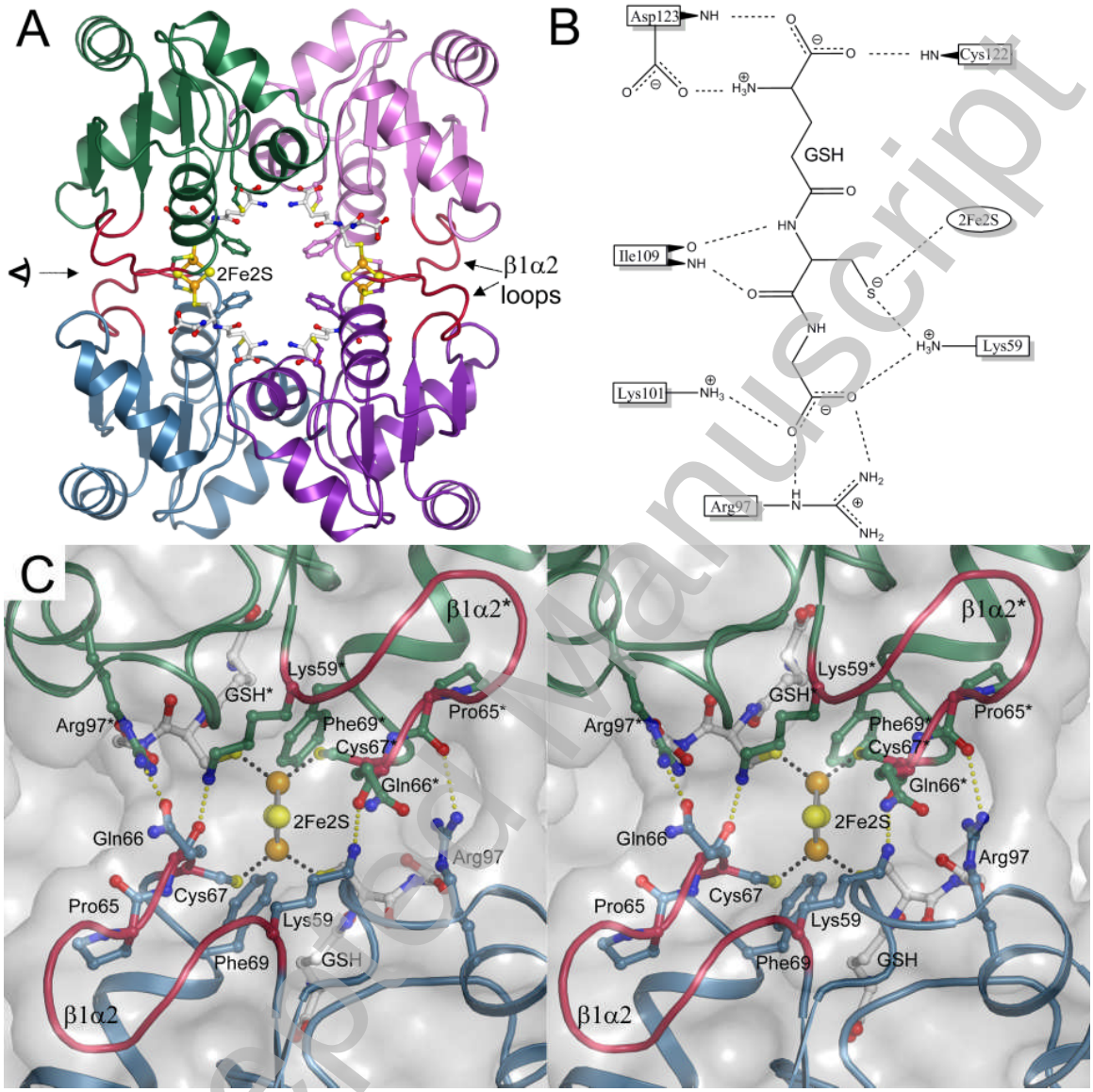

Biochemical Journal Immediate Publication. Published on 29 Oct 2010 as manuscript BJ20101286

FIGURE 5.

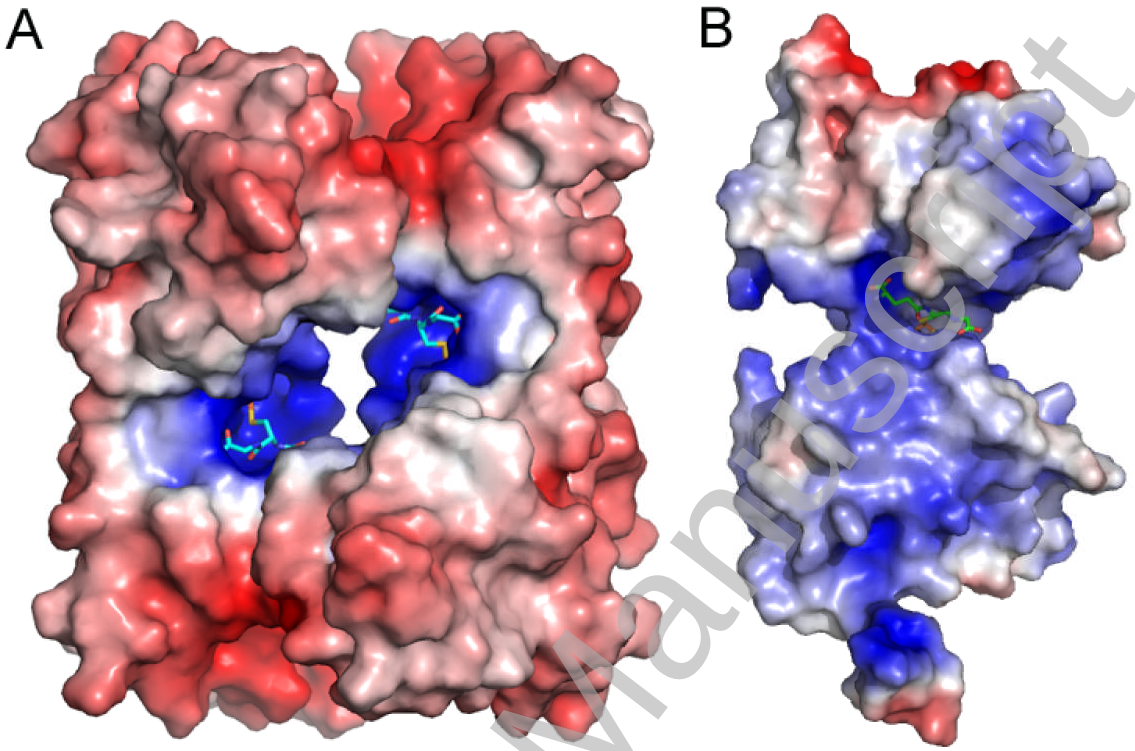

Biochemical Journal Immediate Publication. Published on 29 Oct 2010 as manuscript BJ20101286

FIGURE 6.

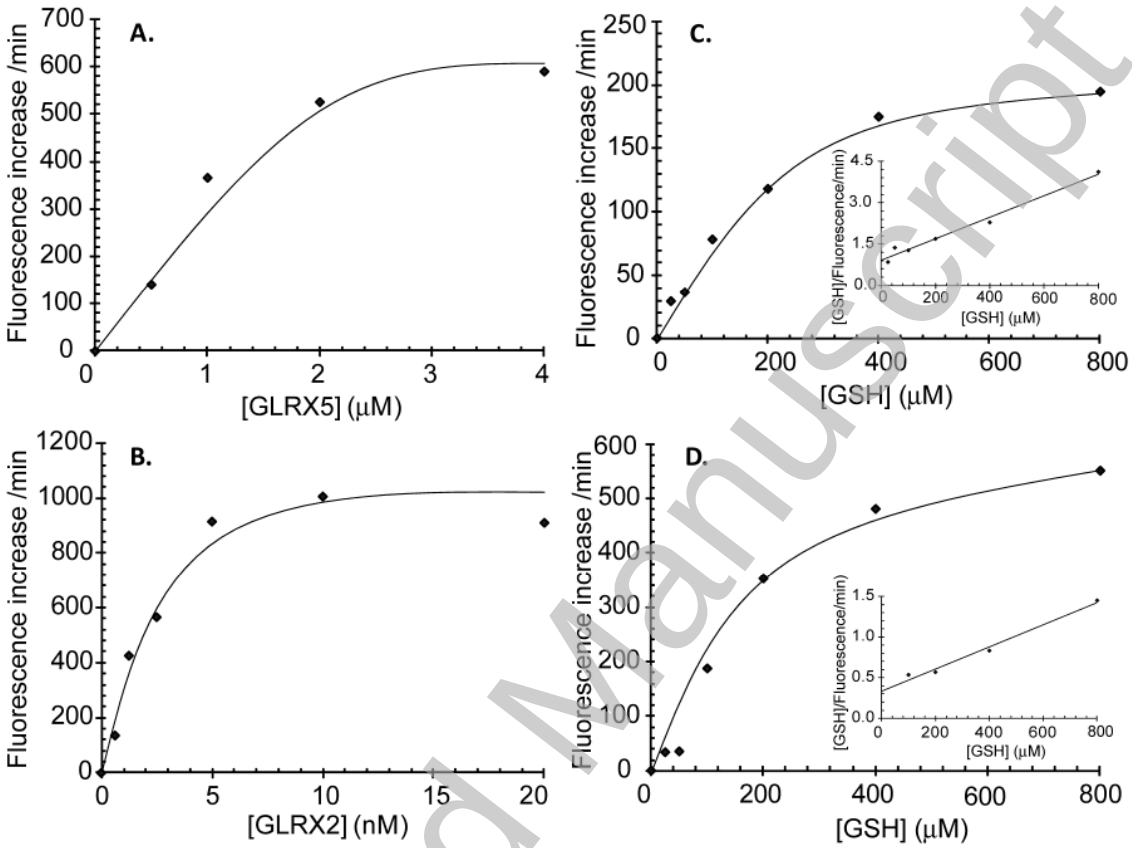

FIGURE 7.